Synthetic and Structural Studies on Group 13 Complexes containing the $M(CO)_3(\eta\text{-}C_5H_5)$ Fragment (M = Cr or Mo). Part 1. Complexes $[E\{M(CO)_3(\eta\text{-}C_5H_5)\}_3]$ (E = In or Tl)†

Lucy M. Clarkson,[a] William Clegg,[a] David C. R. Hockless,[a] Nicholas C. Norman*,[a] and Todd B. Marder*,[b]
[a] Department of Chemistry, The University, Newcastle upon Tyne, NE1 7RU, UK
[b] Department of Chemistry, The University of Waterloo, Waterloo, Ontario N2L 3G1, Canada

The complexes $[E\{M(CO)_3(\eta\text{-}C_5H_5)\}_3]$ (E = In, M = Mo, **1**; E = In, M = Cr, **8**; E = Tl, M = Cr, **5**; E = Tl, M = Mo, **6**) have been prepared and their structures determined by X-ray crystallography. All contain a trigonal-planar indium or thallium centre bonded to three $M(CO)_3(\eta\text{-}C_5H_5)$ fragments (M = Cr or Mo) by unsupported element–element bonds. Synthetic and structural comparisons are made with related complexes and the solution-state properties of all complexes in a variety of solvents are described and discussed. These studies indicate a high degree of ionic character in solution. Extended-Hückel molecular orbital calculations have also been carried out on **1** which confirm the presence of polar In–Mo bonds and also reveal that In–Mo π bonding is quite weak.

In this paper we shall describe some of our studies on complexes of indium and thallium containing the organotransition-metal fragments $M(CO)_3(\eta\text{-}C_5H_5)$ for M = Cr or Mo. This is a continuation of our previous work in this particular area,[1,2] which we will refer to in detail at later stages, and more generally on the chemistry of indium–organotransition metal complexes.[3–5] The area has evolved over many years, and much of it has been described and referenced[1–5] and recently reviewed.[6] In order to put the present study in its proper context, however, we will briefly describe the previous work of other authors on compounds of gallium, indium and thallium which contain the cyclopentadienyl tricarbonylmetal fragment where the metal is chromium, molybdenum or tungsten.

One of the earliest complexes to be described was $[NBu_4][InPh_3\{W(CO)_3(\eta\text{-}C_5H_5)\}]$ by Burlitch and Petersen[7] which, on the basis of infrared spectroscopy, was presumed to contain a direct, unsupported In–W bond. This was in contrast to the aluminium analogue in which the $AlPh_3$ group was bonded to a carbonyl oxygen rather than directly to the tungsten centre. A later and more detailed report by Burlitch *et al.*[8] included additional data on the $GaPh_3$ complex, $[GaPh_3\{W(CO)_3(\eta\text{-}C_5H_5)\}]^-$, together with details on the reactions of EPh_3 (E = Al, Ga or In) with a range of other organotransition-metal anions. Whether or not the Group 13 element was bonded directly to the transition metal or to a carbonyl oxygen was considered to be due to the relative hardness and softness of the respective acidic and basic sites involved. Thus, in CH_2Cl_2, for the tungsten example, aluminium preferred the harder oxygen site whereas indium preferred the softer tungsten; the gallium–tungsten complex was found to exist in both forms in this solvent.

An early report by Hsieh and Mays[9] described the reactions between indium(I) halides and the metal–metal bonded dimers $[M_2(CO)_6(\eta\text{-}C_5H_5)_2]$ (M = Mo or W) which afforded complexes formulated as $[InX\{M(CO)_3(\eta\text{-}C_5H_5)\}_2]$ (X = Cl or Br) although with excess of indium halide the complexes $[InX_2\{M(CO)_3(\eta\text{-}C_5H_5)\}]$ were formed. The dimolybdenum–indium complexes were also produced in the reaction between InCl or InBr and $[Hg\{Mo(CO)_3(\eta\text{-}C_5H_5)\}_2]$. A subsequent report by these authors[10] provided further details on the aforementioned compounds and reactions, together with analytical and infrared data on the trimetal–indium complexes $[In\{M(CO)_3(\eta\text{-}C_5H_5)\}_3]$ (M = Mo or W) obtained by a variety of synthetic routes.

Smith and co-workers[11] have described the reactions between $GaMe_3$ and $[WH(CO)_3(\eta\text{-}C_5H_5)]$ which afforded the complexes $[GaMe_{3-x}\{W(CO)_3(\eta\text{-}C_5H_5)\}_x]$, $x = 1–3$, together with a crystal-structure determination of the tritungsten complex $[Ga\{W(CO)_3(\eta\text{-}C_5H_5)\}_3]$. Subsequent studies by Oliver and co-workers[12] extended this work to the molybdenum system and results from a crystal-structure determination on $[GaMe_2\{W(CO)_3(\eta\text{-}C_5H_5)\}]$ were also presented. Similar work involving thallium has been described by Walther and co-workers.[13]

King[14] reported the synthesis of $[Tl\{Mo(CO)_3(\eta\text{-}C_5H_5)\}_3]$ from the reaction between $Na[Mo(CO)_3(\eta\text{-}C_5H_5)]$ and Tl_2SO_4, and a crystal-structure determination of this complex was subsequently carried out by Rajaram and Ibers.[15] Further work on thallium complexes, particularly thallium(I)–transition metal complexes, was described by Burlitch and Theyson[16] and later by Pedersen and Robinson.[17a] The former authors reported analytical and infrared data on the complexes $[Tl^{III}\{M(CO)_3(\eta\text{-}C_5H_5)\}_3]$ and $[Tl^{I}\{M(CO)_3(\eta\text{-}C_5H_5)\}]$ (M = Cr, Mo and W); the chromium complexes were referred to by the latter authors. We shall discuss the trimetal–thallium complexes in more detail later; the chemistry of thallium(I)–transition metal complexes is an interesting area and one to which we shall return in a future publication.

Ziegler and co-workers[18] have recently described the reaction between $[Mo_2(CO)_6(\eta\text{-}C_5H_5)_2]$ and $InCl_3$ in diglyme (2,5,8-trioxanonane), one product of which contains the anionic complex $[InCl_3\{Mo(CO)_3(\eta\text{-}C_5H_5)\}]^-$, a compound which we have also described,[1] albeit with a different counter cation.

An interesting series of indium and thallium porphyrin complexes has been reported by Guilard and Kadish and co-workers[19] in which the Group 13 element is further bonded to an apical 17-electron metal carbonyl fragment, examples of which include $M(CO)_3(\eta\text{-}C_5H_5)$, M = Cr, Mo or W; X-ray crystal structures have been determined for $[In(oep)\{Mo(CO)_3(\eta\text{-}C_5H_5)\}]$[19c] and $[Tl(oep)\{Mo(CO)_3(\eta\text{-}C_5H_5)\}]$[19b] (oep = 2,3,7,8,12,13,17,18-octaethylporphyrinate).

---

† *Supplementary data available:* see Instructions for Authors, *J. Chem. Soc., Dalton Trans.*, 1991, Issue 1, pp. xviii–xxii.

Non-SI unit employed: eV ≈ 1.60×10^{-19} J.

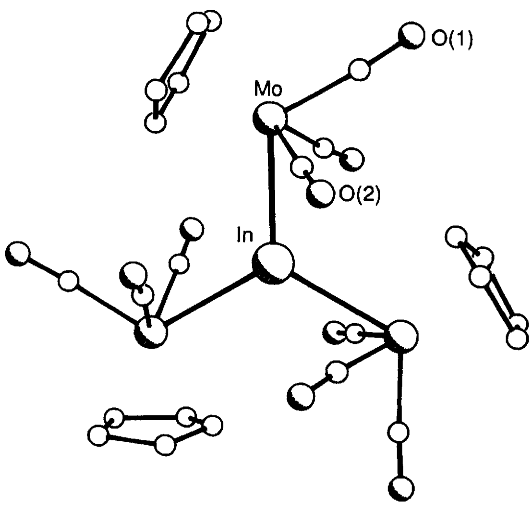

Fig. 1 A view of the molecular structure of complex **1**·thf. Hydrogen atoms omitted for clarity

Table 1 Selected bond lengths (Å) and angles (°) for the complexes $[E\{M(CO)_3(\eta\text{-}C_5H_5)\}_3]$ (E = In, M = Mo, **1**; E = Ga, M = W, **4**; E = In, M = Cr, **8**: E = Tl, M = Cr, **5**; E = Tl, M = Mo, **6**

Compound				
1[a]	In–Mo(1)	2.884(1)	Mo(1)–In–Mo(2)	120.2(1)
	In–Mo(2)	2.887(1)	Mo(1)–In–Mo(3)	119.4(1)
	In–Mo(3)	2.862(1)	Mo(2)–In–Mo(3)	120.4(1)
1·*thf*	In–Mo	2.855(1)	Mo–In–Mo′	120
4[b]	Ga–W(1)	2.744(3)	W(1)–Ga–W(2)	120.0(1)
	Ga–W(2)	2.758(3)	W(1)–Ga–W(3)	119.1(1)
	Ga–W(3)	2.716(3)	W(2)–Ga–W(3)	120.9(1)
8[c]	In–Cr(1)	2.806(1)	Cr(1)–In–Cr(2)	120.6(1)
	In–Cr(2)	2.801(1)	Cr(1)–In–Cr(3)	119.2(1)
	In–Cr(3)	2.775(1)	Cr(2)–In–Cr(3)	120.1(1)
5	Tl–Cr(1)	2.874(2)	Cr(1)–Tl–Cr(2)	120.1(1)
	Tl–Cr(2)	2.852(2)	Cr(1)–Tl–Cr(3)	120.5(1)
	Tl–Cr(3)	2.887(2)	Cr(2)–Tl–Cr(3)	119.2(1)
6[d]	Tl–Mo(1)	3.001(3)	Mo(1)–Tl–Mo(2)	113.92(6)
	Tl–Mo(2)	2.955(3)	Mo(1)–Tl–Mo(3)	122.61(6)
	Tl–Mo(3)	2.938(2)	Mo(2)–Tl–Mo(3)	122.66(6)
6a[e]	Tl–Mo(1)	2.938(1)	Mo(1)–Tl–Mo(2)	120.2(1)
	Tl–Mo(2)	2.917(1)	Mo(1)–Tl–Mo(3)	120.3(1)
	Tl–Mo(3)	2.938(1)	Mo(2)–Tl–Mo(3)	119.5(1)

[a] Crystals from CH_2Cl_2–hexane, data from ref. 1. [b] Data from ref. 11. [c] The only other In–Cr bond distance of which we are aware is for the complex $[InBr(thf)\{Cr(CO)_5\}]$, In–Cr 2.5542(25) and 2.5619(26) Å for two independent molecules,[21] but see following paper. [d] Data from ref. 15, crystals from acetone–pentane. [e] Crystals from CH_2Cl_2–hexane.

Finally we note a preliminary report by Green *et al.*[20] on the synthesis and X-ray structure of $[GaI_2(Et_2O)\{Mo(CO)_3(\eta\text{-}C_5H_4Me)\}]$ formed in the reaction between 'GaI' and $[MoI(CO)_3(\eta\text{-}C_5H_4Me)]$.

In this paper we shall describe our results on the trimetal–indium and -thallium complexes $[E\{M(CO)_3(\eta\text{-}C_5H_5)\}_3]$. Additional work on dimetal- and monometal–indium complexes is described in the following paper.

Results and Discussion

Table 2 Atomic coordinates (× 10^4) for complex **1**·thf

Atom	*x*	*y*	*z*
In	6 667	3 333	7 500
Mo	5 014(1)	4 395(1)	7 500
C(1)	3 179(8)	3 230(10)	7 500
O(1)	2 065(7)	2 590(9)	7 500
C(2)	4 835(5)	3 392(4)	6 181(5)
O(2)	4 689(6)	2 856(5)	5 377(4)
C(3)	6 773(9)	6 352(24)	7 500
C(4)	6 164(17)	6 381(6)	6 685(9)
C(5)	4 889(9)	6 171(7)	6 990(10)
C(6)	1 224(108)	10 541(136)	5 000

(*i*) *Synthesis*.—In a previous paper[1] we described the preparation of the trimolybdenum–indium complex $[In\{Mo(CO)_3(\eta\text{-}C_5H_5)\}_3]$ **1**, from the reaction between $InCl_3$ and 3 equivalents of $Na[Mo(CO)_3(\eta\text{-}C_5H_5)]$ in tetrahydrofuran (thf) solution. The tritungsten complex $[In\{W(CO)_3(\eta\text{-}C_5H_5)\}_3]$ **2** was prepared similarly. Hsieh and Mays[10] reported the preparation of **1** and **2** by essentially the same method together with alternative syntheses involving the reactions between $InCl_3$ and $Na[M(CO)_3(\eta\text{-}C_5H_5)]$ in water, between $[Hg\{M(CO)_3(\eta\text{-}C_5H_5)\}_2]$ and indium metal and between $InMe_3$ and $[MH(CO)_3(\eta\text{-}C_5H_5)]$ (M = Mo or W). The gallium complexes $[Ga\{M(CO)_3(\eta\text{-}C_5H_5)\}_3]$ (M = Mo, **3**; or W, **4**) have also been prepared similarly using $GaMe_3$ as described in the Introduction.[11,12]

The trimetal–thallium complexes $[Tl\{M(CO)_3(\eta\text{-}C_5H_5)\}_3]$ (M = Cr, **5**; Mo, **6**; or W, **7**) were prepared by Burlitch and Theyson[16] from the reactions between $TlCl_3{\cdot}4H_2O$ and $3[M(CO)_3(\eta\text{-}C_5H_5)]^-$ in thf but are also formed upon disproportionation of the thallium(I) complexes $[Tl\{M(CO)_3(\eta\text{-}C_5H_5)\}]$[16,17] in solution. In addition, **5** is formed in high yield from the reaction between $[Cr_2(CO)_6(\eta\text{-}C_5H_5)_2]$ and either excess of thallium metal in benzene[17a] or thallium(I) acetate in refluxing ethanol.[17b] King's route[14] to **6** was mentioned in the Introduction whilst Manning and co-workers[17b] have also synthesised this complex from $[Mo_2(CO)_6(\eta\text{-}C_5H_5)_2]$ and thallium(I) acetate, *cf.* their route to **5**.

We have prepared complex **5** {Tl metal, $[Cr_2(CO)_6(\eta\text{-}C_5H_5)_2]$}[17a] and **6** (disproportionation of $[Tl\{Mo(CO)_3(\eta\text{-}C_5H_5)\}]$ in thf),[16] in order to examine their solid- and solution-state properties (see below), together with the new trichromium–indium complex $[In\{Cr(CO)_3(\eta\text{-}C_5H_5)\}_3]$ **8**, from the reaction between $InCl_3$ and 3 equivalents of $Na/K[Cr(CO)_3(\eta\text{-}C_5H_5)]$ in thf. Further details are given in the Experimental section.

(*ii*) *Structures*.—In ref. 1 we reported the crystal and molecular structure of complex **1**, the crystals having been obtained by diffusion of hexane into a CH_2Cl_2 solution of **1** at −20 °C over a period of days. Crystals of the tungsten–gallium complex **4** obtained from methylcyclohexane are isomorphous.[11] Although there is no crystallographically imposed symmetry, **1** and **4** possess approximate C_{3h} molecular symmetry as illustrated in structure diagram **A**. In the course of our studies we have also determined the structures of **1** obtained by solvent diffusion from thf–hexane, the trichromium–indium and -thallium complexes, **8** and **5**, and the trimolybdenum–thallium complex **6** from a different solvent system from that previously reported[15] for this complex.

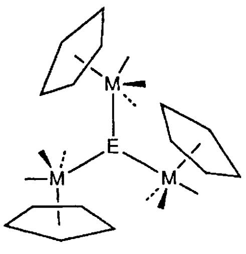

A

The crystals of complex **1** obtained from CH_2Cl_2–hexane mixtures were yellow plates containing no solvent of crystallisation.[1] Crystals obtained from thf–hexane, however, were

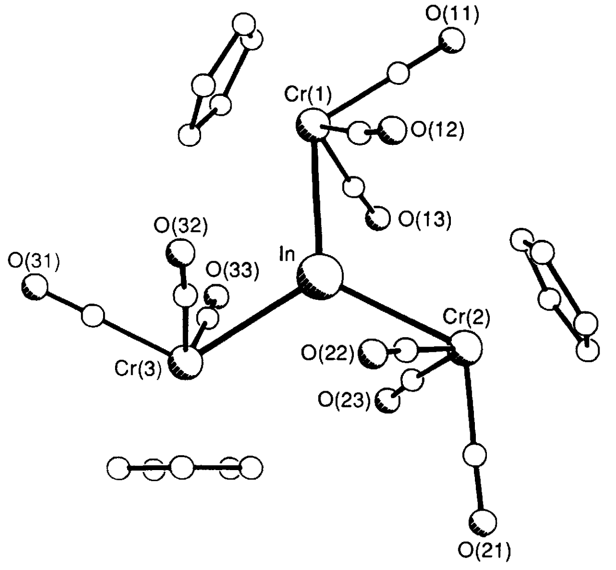

Fig. 2 A view of the molecular structure of complex **8**. Hydrogen atoms omitted for clarity

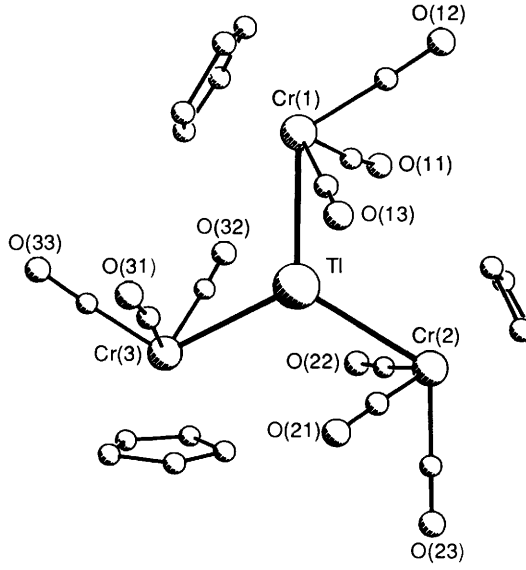

Fig. 3 A view of the molecular structure of complex **5**. Hydrogen atoms omitted for clarity

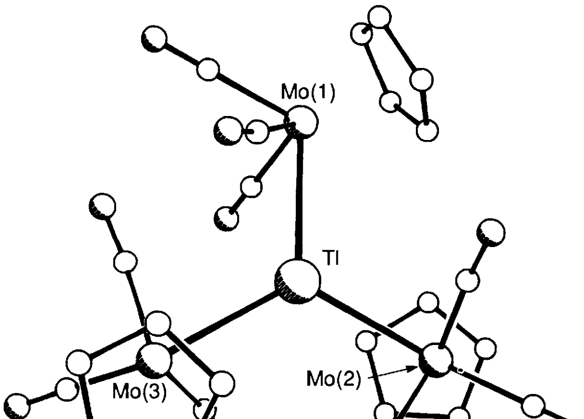

Fig. 4 A view of the molecular structure of complex **6** redrawn from coordinates in ref. 15. Crystals from acetone–pentane

Table 3 Atomic coordinates (× 10^4) for complex **8**

Atom	*x*	*y*	*z*
In	6 341(1)	6 503(1)	3 296(1)
Cr(1)	4 636(1)	5 343(1)	2 493(1)
Cr(2)	5 526(1)	7 936(1)	3 849(1)
Cr(3)	8 849(1)	6 232(1)	3 480(1)
C(11)	2 972(4)	5 544(3)	2 168(4)
O(11)	1 925(3)	5 673(2)	1 966(4)
C(12)	4 479(4)	5 644(2)	3 734(3)
O(12)	4 284(5)	5 786(2)	4 510(3)
C(13)	4 636(4)	6 171(3)	1 653(3)
O(13)	4 556(4)	6 665(2)	1 071(3)
C(14)	5 327(7)	4 563(3)	1 484(4)
C(15)	4 250(5)	4 281(4)	1 634(6)
C(16)	4 404(6)	4 110(3)	2 612(6)
C(17)	5 619(6)	4 294(3)	3 094(4)
C(18)	6 185(4)	4 582(2)	2 361(4)
C(21)	6 601(4)	8 724(2)	4 337(3)
O(21)	7 266(4)	9 230(2)	4 632(3)
C(22)	6 414(4)	7 399(3)	4 930(3)
O(22)	6 923(4)	7 114(2)	5 667(2)
C(23)	6 287(3)	8 002(2)	2 783(3)
O(23)	6 717(3)	8 108(2)	2 106(2)
C(24)	3 788(4)	8 303(3)	2 853(4)
C(25)	4 080(4)	8 810(3)	3 627(5)
C(26)	4 077(5)	8 425(4)	4 507(5)
C(27)	3 784(5)	7 652(4)	4 267(5)
C(28)	3 598(4)	7 572(3)	3 240(5)
C(31)	9 420(4)	5 275(3)	3 234(4)
O(31)	9 779(4)	4 668(2)	3 103(5)
C(32)	8 187(4)	5 673(3)	4 377(4)
O(32)	7 876(4)	5 304(3)	4 980(3)
C(33)	7 997(4)	6 155(3)	2 168(3)
O(33)	7 569(4)	6 108(3)	1 323(3)
C(34)	9 471(5)	7 393(3)	3 172(5)
C(35)	10 387(5)	6 887(3)	3 136(6)
C(36)	10 772(4)	6 549(3)	4 034(6)
C(37)	10 022(7)	6 879(4)	4 690(5)
C(38)	9 237(4)	7 406(3)	4 078(4)

clear yellow rods which quickly became opaque after removal from the mother-liquor; this observation clearly indicated a different crystal structure. Accordingly, we carried out a structure determination on these crystals (hereafter **1**•thf), the results of which are shown in Fig. 1 and Tables 1 and 2. Crystallographic, intensity-data collection and structure-solution parameters for this and all subsequent structures are given in the Experimental section. The results show that the molecular structure of **1**•thf is the same as for **1** but in this case the approximate C_{3h} symmetry found in the previous structure is now crystallographically imposed. A molecule of thf is present as solvent of crystallisation although there are no significantly close intermolecular contacts. The important bond lengths and angles for **1** and **1**•thf are compared in Table 1 but the differences between the two structures are not particularly significant, although the In–Mo bond lengths are somewhat shorter in **1**•thf than in **1**.

The structures of the chromium complexes **8** and **5**, in crystals obtained from CH_2Cl_2–hexane, are shown in Figs. 2 and 3 respectively. Bond lengths and angles for both structures are given in Table 1 and atomic positional parameters are presented in Tables 3 and 4. Both structures are isomorphous with **1**, from CH_2Cl_2–hexane, and **4**, and thus are of type **A**.

As mentioned in the Introduction, the structure of complex **6** was reported by Rajaram and Ibers,[15] the crystals having been obtained from acetone–pentane mixtures. A view of this structure is shown in Fig. 4. It is different from the structures of **1**, **4**, **5** and **8** with respect to the conformations about the metal–metal bonds, as is evident from a comparison of the relevant Figures and from diagrams **A** and **B**. Thus in **6**, two of the $Mo(CO)_3(\eta\text{-}C_5H_5)$ fragments are rotated approximately 90°

Table 4 Atomic coordinates (× 10^4) for complex **5**

Atom	*x*	*y*	*z*
Tl	1344(1)	1499(1)	3314(1)
Cr(1)	544(1)	2965(1)	3905(1)
Cr(2)	3885(1)	1224(1)	3439(1)
Cr(3)	−417(1)	329(1)	2464(1)
C(11)	1291(8)	3050(5)	2847(7)
O(11)	1696(7)	3177(4)	2152(5)
C(12)	1616(11)	3751(6)	4366(7)
O(12)	2231(9)	4277(5)	4632(7)
C(13)	1479(9)	2452(5)	5003(7)
O(13)	2015(9)	2163(5)	5734(5)
C(14)	−1171(11)	2650(8)	4354(10)
C(15)	−1330(9)	2576(7)	3320(11)
C(16)	−1196(9)	3287(6)	2923(10)
C(17)	−927(10)	3795(7)	3721(11)
C(18)	−873(12)	3415(7)	4591(10)
C(21)	3302(10)	638(7)	4331(10)
O(21)	3019(10)	237(6)	4925(9)
C(22)	3013(10)	1142(6)	2132(7)
O(22)	2540(9)	1078(6)	1302(6)
C(23)	4476(11)	279(6)	3191(11)
O(23)	4884(10)	−303(5)	3050(10)
C(24)	4205(11)	2404(7)	4066(10)
C(25)	4444(12)	2401(6)	3139(12)
C(26)	5378(12)	1901(7)	3082(12)
C(27)	5781(9)	1582(6)	3989(13)
C(28)	5049(15)	1905(10)	4656(10)
C(31)	−618(10)	629(5)	3709(8)
O(31)	−813(11)	755(5)	4485(6)
C(32)	−431(9)	1169(5)	1633(7)
O(32)	−479(10)	1654(5)	1041(7)
C(33)	−2060(10)	536(6)	2134(9)
O(33)	−3103(7)	666(5)	1904(8)
C(34)	549(13)	−713(5)	3058(9)
C(35)	1133(9)	−422(5)	2380(9)
C(36)	336(13)	−415(6)	1464(8)
C(37)	−722(13)	−712(8)	1548(13)
C(38)	−643(12)	−905(5)	2510(13)

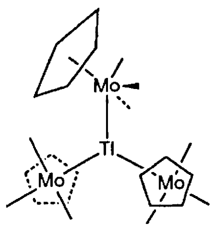

B

with respect to structure **A** such that the Mo_3Tl mean plane is perpendicular to the symmetry plane of these two fragments. In **A** the M_3E plane is coplanar with the symmetry plane of all three $M(CO)_3(\eta\text{-}C_5H_5)$ fragments, an observation to which we will return later. Moreover, the thallium atom is significantly displaced from the plane defined by the three molybdenum atoms (0.586 Å)[15] to an extent whereby the co-ordination geometry around the thallium centre was described as trigonal pyramidal.[15] In the compounds which adopt structure **A** the indium or thallium centres are much more nearly coplanar with the M_3 plane [mean displacements: 0.017, **1**;[1] 0, **1**·thf; 0.002, **4**;[11] 0.028, **8**; 0.060 Å, **5**]. It was curious that **6** should adopt a different structure from all the other related compounds and so when, during the course of our work on thallium(I)–transition metal complexes, we obtained crystals of **6** from CH_2Cl_2–hexane mixtures we were interested to see whether the structure would be of type **B**, *i.e.* the same as previously observed for **6**, or of type **A** as found for **5** and for **1** and **8**, all of which were obtained from CH_2Cl_2–hexane. The results, shown in Fig. 5 and presented in Tables 1 and 5, clearly show that **6** from the CH_2Cl_2–hexane solvent system (hereafter **6a**) crystallises with the type **A** structure. In fact, the crystals are isomorphous with **1**, **4**, **5** and **8**. Thus **6** crystallises in two different polymorphs, depending on the solvents used for crystallisation, which have structures differing in the conformations about the Tl–Mo bonds in a manner which we have previously described. It is likely that the two crystal structures, neither of which contains any solvent, are close in energy and the precise structure adopted is influenced by solvent–solute interactions during crystallisation. We suspect, also, that polymorphism in these and related systems is much more common than is currently realised. X-Ray crystal-structure determinations are not normally carried out more than once on a particular compound but, as we have seen here, crystals obtained from different solvents may well have different structures, even in the absence of any solvent of crystallisation, which in turn may result in slightly different molecular structures. In **6a** the thallium is markedly less pyramidal than in **6**, the displacement from the Mo_3 plane being 0.045 Å (*cf.* 0.586 Å for **6**) but similar to **5** (0.060 Å). The different conformations about the Tl–Mo bonds and the pyramidality, or lack of it, at the thallium centre for **6** and **6a**, *i.e.* the *same* compound, serve to remind us of how careful we must be when seeking to account for any observations such as these based on the results from a single crystal-structure determination, *especially* when the energy differences between various alternatives are likely to be small.

With this warning in mind we shall now consider the bonding in the M_3E complexes, specifically the extent of any M–E π bonding, based on the results from extended-Hückel molecular orbital (EHMO) calculations.

(*iii*) *Bonding.*—The X-ray structures of the trimetal–indium and –thallium complexes described in the previous section are the only ones which have been reported in the literature with the exception of the tricobalt–indium complex, $[In\{Co(CO)_4\}_3]$.[22] There are, however, a number of related and formally isoelectronic complexes involving elements from Groups 14–16 which have been structurally characterised. Cassidy and Whitmire[23] have described the dianionic triiron–tin and –lead complexes $[E\{Fe(CO)_4\}_3]^{2-}$ (E = Sn or Pb) which are isostructural with $[In\{Co(CO)_4\}_3]$, Huttner *et al.*[24] have reported the anionic trichromium–antimony complex $[Sb\{Cr(CO)_5\}_3]^-$ and Herberhold *et al.*[25] have characterised the trimanganese–tellurium complex $[Te\{Mn(CO)_2(\eta\text{-}C_5H_5)\}_3]$. The extent of π bonding which exists between the main-group and transition-element centres is something which the authors discussed, and to which we have drawn attention in a recent review.[6] Clearly, the extent of π bonding will vary from compound to compound, and it will be interesting to look closely at the entire range of known complexes but at this time we shall restrict ourselves to a discussion of the bonding in **1** based on results obtained from EHMO calculations.

The calculations were performed on complex **1** with idealised C_{3h} symmetry. Bond distances and angles were obtained by averaging the values from the structure determination[1] as deviations from the idealised symmetry were small. Important geometric parameters used were: In–Mo 2.878, Mo–C_5H_5 ring centroid 1.896, Mo–C(O) 1.970, C–O 1.192 Å; In–Mo–C_5H_5 centroid 120.0, In–Mo-unique CO 121.3°. The C_5H_5 rings were constructed with D_{5h} symmetry and the CO ligands linear. Calculations were also performed on the $\{Mo(CO)_3(\eta\text{-}C_5H_5)\}_3{}^{3-}$ fragment and on an isolated $[Mo(CO)_3(\eta\text{-}C_5H_5)]^-$ anion using the above geometric parameters.

For $[Mo(CO)_3(\eta\text{-}C_5H_5)]^-$, the three highest occupied orbitals correspond to the d^6 configuration and are of σ, δ and π symmetry with respect to the indium atom. The calculated energies are −11.05, −11.68 and −11.73 eV respectively and they are of approximately 45–50% Mo character with the remainder being largely CO π^*.[26] The above orbitals are numbered in order of increasing stability: $\sigma(28)$, $\delta(29)$, $\pi(30)$.

When the three $[Mo(CO)_3(\eta\text{-}C_5H_5)]^-$ anions are combined

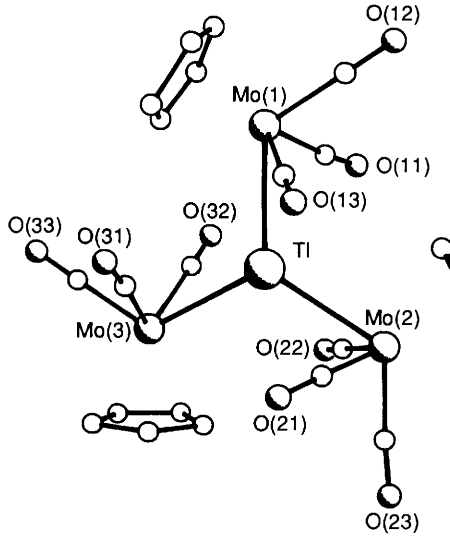

Fig. 5 A view of the molecular structure of complex **6a**. Hydrogen atoms omitted for clarity. Crystals from CH_2Cl_2–hexane

Table 5 Atomic coordinates (× 10^4) for complex **6a**

Atom	*x*	*y*	*z*
Tl	1313(1)	1436(1)	3274(1)
Mo(1)	530(1)	2896(1)	3913(1)
Mo(2)	3834(1)	1150(1)	3382(1)
Mo(3)	−444(1)	282(1)	2426(1)
C(11)	1365(8)	2994(5)	2758(7)
O(11)	1766(7)	3093(4)	2076(6)
C(12)	1634(10)	3732(5)	4408(8)
O(12)	2223(9)	4233(5)	4663(7)
C(13)	1578(9)	2361(6)	5028(6)
O(13)	2151(8)	2083(5)	5737(5)
C(14)	−1256(12)	2586(8)	4370(12)
C(15)	−1443(9)	2555(7)	3300(9)
C(16)	−1296(10)	3267(8)	2959(9)
C(17)	−1005(10)	3756(7)	3792(11)
C(18)	−962(12)	3335(9)	4662(11)
C(21)	3197(10)	527(6)	4345(8)
O(21)	2907(9)	137(7)	4941(9)
C(22)	2898(8)	983(5)	2011(8)
O(22)	2388(9)	911(5)	1170(6)
C(23)	4467(10)	159(5)	3130(10)
O(23)	4879(9)	−408(5)	3025(10)
C(24)	4225(9)	2394(6)	3980(9)
C(25)	4447(11)	2346(6)	3018(11)
C(26)	5373(10)	1881(6)	3010(12)
C(27)	5765(9)	1588(6)	3950(12)
C(28)	5030(14)	1924(8)	4610(10)
C(31)	−656(10)	629(5)	3751(7)
O(31)	−825(9)	767(5)	4542(6)
C(32)	−530(8)	1170(5)	1559(6)
O(32)	−612(9)	1681(5)	1023(6)
C(33)	−2157(11)	485(6)	2102(10)
O(33)	−3152(7)	593(5)	1928(8)
C(34)	563(12)	−822(6)	3008(8)
C(35)	1112(9)	−533(5)	2280(9)
C(36)	359(11)	−537(6)	1375(8)
C(37)	−701(11)	−811(6)	1485(10)
C(38)	−599(11)	−1001(6)	2496(11)

in the C_{3h} arrangement found in complex **1** the Mo···Mo separations are 4.98 Å. Thus there is relatively little interaction between the individual molybdenum fragments, the total energy of the $\{Mo(CO)_3(\eta\text{-}C_5H_5)\}_3{}^{3-}$ unit (abbreviated to $Mo_3{}^{3-}$) being about 0.7 eV higher than that of the sum of three isolated $[Mo(CO)_3(\eta\text{-}C_5H_5)]^-$ anions probably due to non-bonded contacts. The magnitude of the reduced overlap population between each pair of Mo atoms is less than 0.001. In the isolated $[Mo(CO)_3(\eta\text{-}C_5H_5)]^-$ anion the charge on Mo is +0.76 and in the Mo_3 trianionic unit, $Mo_3{}^{3-}$, the charge on each Mo atom is +0.75.

In C_{3h} symmetry, indium s transforms as a′, $p_{x,y}$ as e′ and p_z as a″. Thus there will be no match for orbitals of e″ symmetry on the Mo_3 unit. The a′ and e′ combinations will be of σ *symmetry* and a″ of π symmetry. The $\{Mo(CO)_3(\eta\text{-}C_5H_5)\}_3{}^{3-}$ fragment orbitals are shown on the right-hand side of Fig. 6 and are derived as follows. Combining the three sets of the highest-lying occupied orbitals of $[Mo(CO)_3(\eta\text{-}C_5H_5)]^-$, σ(28), δ(29) and π(30), will provide a total of nine molecular orbitals which are largely of Mo d character. Thus the three σ orbitals (28) split into the 3a′ (σ) and 3e′ (σ) levels at −11.17 and −11.05 eV respectively. The three δ orbitals (29) also split into a′ and e′ levels, 2a′(δ) and 2e′(δ). However, these are inappropriate in orientation to become involved in bonding to the indium centre and are therefore largely non-bonding. The three π orbitals (30) split into 2e″ (π) and 2a″ (π), the former of which is strictly non-bonding by symmetry. There is a series of orbitals labelled 1a′, 1e′, 1a″ and 1e″ at around −12.6 eV which are Mo–C_5H_5 bonding orbitals largely localised on the C_5H_5 rings. However, we include these in our discussion as the 1a′ (σ) orbital at −12.65 eV will become important in bonding with In s at −12.60 eV.

Due to the large energy separation between the In 5s and 5p orbitals there is little mixing between them and the bonding between the In^{3+} and $\{Mo(CO)_3(\eta\text{-}C_5H_5)\}_3{}^{3-}$ fragments can be treated by examination of the σ bonding to the In s level, σ bonding to In $p_{x,y}$ e′ and π bonding to In p_z a″.

For the molecule **1** the energy levels are shown in the centre of Fig. 6. The important a′ σ interactions generate two low-lying molecular orbitals 1a′ and 2a′ at −12.72 and −12.60 eV. They are composed largely of In s and Mo_3 1a′ character with a modest contribution from the much higher-lying Mo_3 3a′ orbital. As pointed out earlier, the Mo_3 2a′ orbital has δ symmetry and does not mix efficiently with the other a′ levels. The remaining σ interaction is of e′ symmetry and is the highest occupied molecular orbital (HOMO), 3e′ lying at −11.19 eV. It is derived from the stabilisation of the HOMO of the $Mo_3{}^{3-}$ fragment, 3e′ (−10.99 eV), by interaction with In $p_{x,y}$. The energy mismatch of 4.8 eV between In p and the Mo_3 3e′ level leads to the largely molybdenum character of the molecular HOMO and a final In $p_{x,y}$ atomic orbital occupation of about 0.21 e^-.

Finally, we address the question of π bonding to In p_z. Interaction of In p_z with Mo_3 2a″ (π) leads to a weak π bond and the stabilisation of Mo_3 2a″ (π) by about 0.07 eV. Again, this interaction is small due to the energy mismatch between the orbitals such that the atomic orbital occupation for In p_z in **1** is calculated to be only 0.12 e^-.

The final calculated charges are +0.97 on each Mo atom and +1.55 on In, and the reduced overlap population between In and each Mo is 0.198.

Clearly the bonding between In and Mo is quite polar and therefore consistent with the observed dissociation of $[Mo(CO)_3(\eta\text{-}C_5H_5)]^-$ from **1** in polar co-ordinating solvents as described in ref. 1 and in the following section. There is evidence for π bonding between In and Mo but the presence of three strong π-acceptor CO ligands on each molybdenum fragment and the high energy of the In p level mitigate the strength of this interaction. Interestingly, as noted in ref. 1, the orientation of each $Mo(CO)_3(\eta\text{-}C_5H_5)$ fragment with respect to the $InMo_3$ plane does serve to maximise the degree of π bonding between In and Mo. Thus rotation about the In–Mo bond by 90° would bring a lower-lying molybdenum orbital into appropriate orientation for π bonding. However, this level has only 20% molybdenum character, the remainder being localised on the C_5H_5 ring, and this factor together with its lower energy means that it is less well disposed towards π bonding.[26] A further point concerns the orientation of the Mo-based fragment orbitals. The σ-bonding orbitals on Mo are

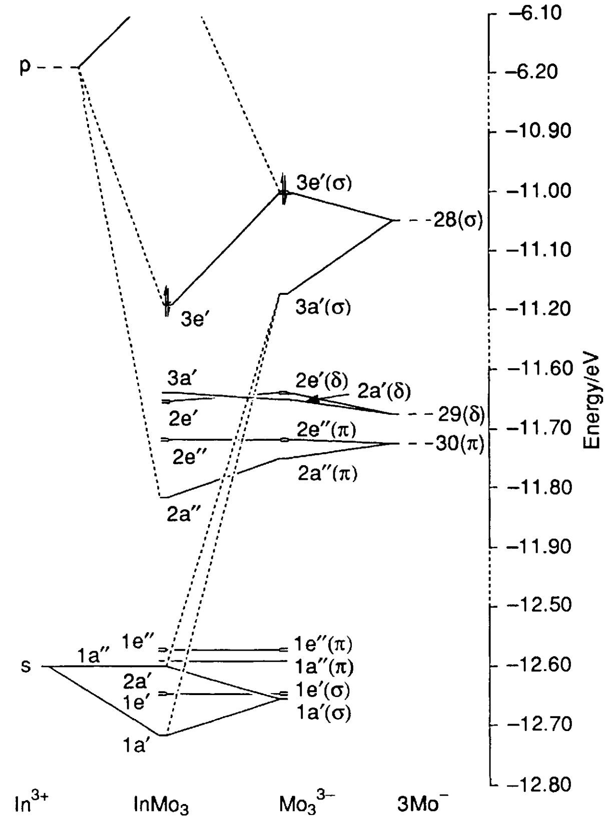

Fig. 6 Important orbital interactions in complex **1** as derived from EHMO calculations. Orbitals are labelled as described in the text

essentially aligned with the In–Mo vectors for maximum overlap however, the π orbitals on Mo leading to Mo_3 2a″ (π) and the 2a″ π-bonding level in **1** are rotated 30° with respect to the In–Mo vectors as shown in **C**. Thus the molybdenum orbitals of interest are a mixture of d_{xz} and d_{yz} and lie parallel to each C_5H_5 ring such that on Mo(3) this is almost a pure d_{yz} orbital. This reflects a geometric distortion which is evident in the crystal structure of **1** such that the two *cis* carbonyls (with respect to In) on each molybdenum fragment subtend angles of *ca.* 66.8° to the indium atom whilst the angle to the *trans* carbonyl is *ca.* 80.9°. We suspect that this canting of the $Mo(CO)_3(\eta\text{-}C_5H_5)$ fragments results from an intramolecular steric interaction between one of the C_5H_5 C–H bonds on one fragment with these two *cis* carbonyls on an adjacent fragment, the H···C(O) and H···O contacts being around 2.52 and 2.72 Å respectively in the idealised C_{3h} structure used in the calculations. This is shown diagrammatically in **D**. In the structure of complex **1**[1] close contacts are observed between H(34) and O(23) (2.68 Å) and between H(27) and O(12) (2.62 Å).

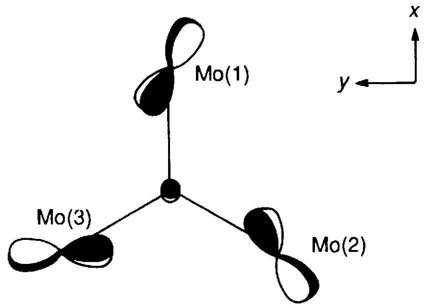

C

In summary, therefore, these calculations indicate that In–Mo π bonding is relatively weak. In complex **1** this is partly due to a poor geometrical alignment of the π-type orbitals involved, as shown in **C**, but more generally, and probably more importantly, to the large energy mismatch between the metal-based orbitals and In 5p. Moreover, in **1**, any multiple bonding which is present is certainly not reflected in the In–Mo bond distances observed. In **1** and **1**·thf the In–Mo bond lengths are 2.878 (av.) and 2.855(1) Å respectively which are of the same order as those observed in other In–Mo complexes: $[Na(thf)_2][InCl_2\{Mo(CO)_3(\eta\text{-}C_5H_5)\}_2]$ 2.850 (av.),[1] $[Na(thf)_2][InCl_3\{Mo(CO)_3(\eta\text{-}C_5H_5)\}]$ 2.739(1),[1] $[InCl(thf)\{Mo(CO)_3(\eta\text{-}C_5H_5)\}_2]$ 2.824 (av.)[2] and $[In(oep)\{Mo(CO)_3(\eta\text{-}C_5H_5)\}]$ 2.890(1) Å.[19c] Two other structures containing In–Mo bonds have recently been published:[27] $[(OC)_5MSn(OBu^t)_3\text{-}InMo(CO)_5]$ [M = Cr, In–Mo 2.734(2); M = Mo, In–Mo 2.742(1) Å].

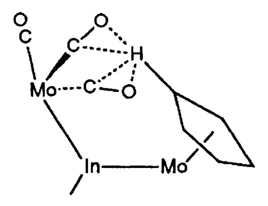

D

It is clear from the calculations that, in general, In–ML_n bonds are quite polar, with considerable positive character on indium and a build up of negative charge on the ML_n fragments. This is entirely consistent with the ionic behaviour of such compounds in solution (see below).

As a final comment we draw attention to two other complexes, namely $[In\{Fe(CO)_2(\eta\text{-}C_5H_5)\}_3]$[3] and $[Te\{Mn(CO)_2(\eta\text{-}C_5H_5)\}_3]$.[25] These are strictly isoelectronic and yet are usually drawn in rather different ways,[6] **E** and **F**. Although these representations primarily reflect an electron-counting formalism, the presence of π or multiple bonding in the tellurium complex is clearly implied. Our calculations on **1** have shown that π bonding to indium is weak due to the high energy of In 5p orbital and therefore drawings such as **A** and **E** are probably faithful representations of the bonding in these complexes. Tellurium, however, is much more electronegative than indium and thus the 5p level of Te is more stable, lying closer in energy to the ML_n frontier orbitals. We would therefore expect that π bonding to tellurium in $[Te\{Mn(CO)_2(\eta\text{-}C_5H_5)\}_3]$ and related complexes[6] will be considerably stronger than that to indium. The bonding implied in **F** is also likely to be a faithful representation.

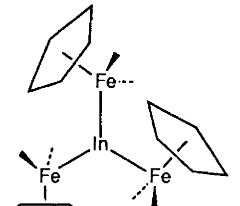

E

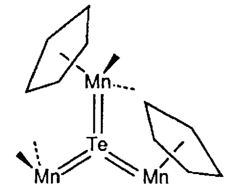

F

(*iv*) *Solution Studies.*—In our original report on the synthesis and solution-state properties of complex **1** we presented data on the extent of dissociation in various solvents.[1] In brief, we stated that the infrared spectra in the carbonyl stretching region were consistent with **1** being fully associated in CH_2Cl_2 and toluene, *i.e.* retaining the structure found in the solid state, being partially dissociated in thf and fully dissociated in MeCN.[1] In the case of MeCN we assumed that dissociation occurred to give $[In(MeCN)_x]^{3+}$ and $3[Mo(CO)_3(\eta\text{-}C_5H_5)]^-$ since the frequencies and intensities observed for **1** in this solvent (1897 and 1777 cm^{-1})[1] are very similar to those found, in thf, for $[N(PPh_3)_2][Mo(CO)_3(\eta\text{-}C_5H_5)]$ [1897 and 1781 cm^{-1}, Fig.

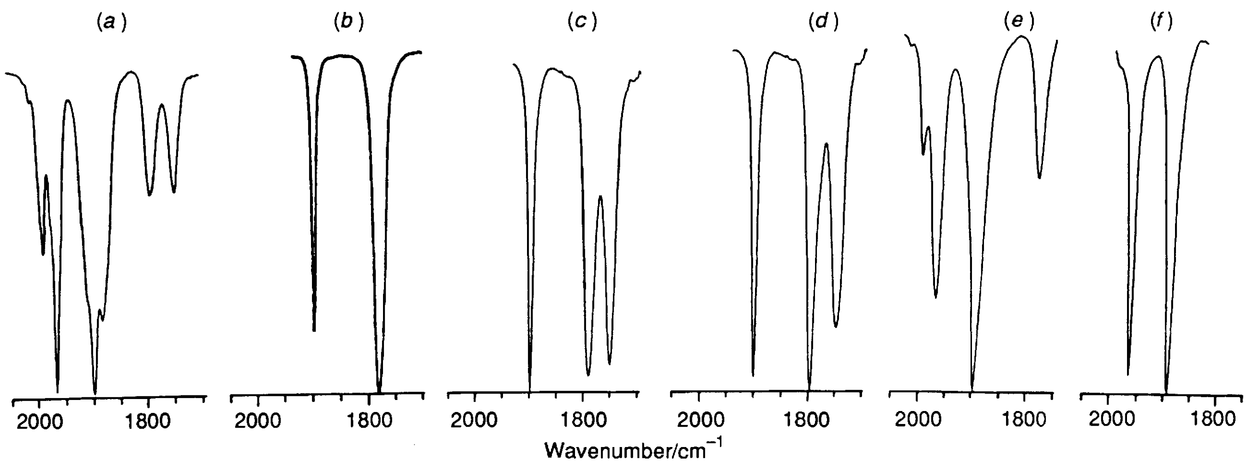

Fig. 7 Infrared spectra in the carbonyl stretching region in thf (unless otherwise stated): (*a*) complex **1**, KBr cells; (*b*) $[N(PPh_3)_2][Mo(CO)_3(\eta\text{-}C_5H_5)]$; (*c*) $K[Mo(CO)_3(\eta\text{-}C_5H_5)]$; (*d*) $Na[Mo(CO)_3(\eta\text{-}C_5H_5)]$; (*e*) **1** in acetone; (*f*) **1**, CaF_2 cells

Table 6 Infrared spectroscopic data [$\nu(CO)/cm^{-1}$] for the complexes

Compound		
1	$[In\{Mo(CO)_3(\eta\text{-}C_5H_5)\}_3]$	1989m, 1967s, 1898s, 1880m, 1789m, 1749m[a–c]
		1996m, 1968s, 1897s, 1781m[d–f]
		1994m, 1968s, 1895s, 1777m[e,g]
		1970s, 1956s, 1877s[h]
		1965s, 1894s[a,e]
8	$[In\{Cr(CO)_3(\eta\text{-}C_5H_5)\}_3]$[i]	2011w, 1957s, 1887s[e,j]
		2011w, 1954s, 1920w, 1889s[e,k]
		2009w, 1985w, 1955s, 1888s[a,e,l]
		1955s, 1880s, 1774m[e,g]
		2010w, 1978m, 1955s, 1892s, 1778m[d,e]
		2019w, 1978s, 1955s, 1895s, 1881s, 1792m, 1746m[a,b,m]
5	$[Tl\{Cr(CO)_3(\eta\text{-}C_5H_5)\}_3]$[e,n]	2010w, 1990w, 1949s, 1897s[j]
		2011w, 1990w, 1948s, 1920w, 1896s[k]
		2007w, 1989w, 1948s, 1918w, 1896s[a]
		2005w, 1987w, 1947s, 1895s, 1774w[g]

[a] Recorded in thf solution. [b] Recorded in KBr solution cells. [c] See Fig. 7(*a*). [d] Recorded in acetone solution. [e] Recorded in CaF_2 cells. [f] See Fig. 7(*e*). [g] Recorded in MeCN solution. [h] Recorded as a KBr disc. [i] See Fig. 8. [j] Recorded in CH_2Cl_2 solution. [k] Recorded in toluene solution. [l] See Fig. 8(*c*). [m] See Fig. 8(*f*). [n] See Fig. 9.

7(*b*)], *i.e.* a situation which involves free $[Mo(CO)_3(\eta\text{-}C_5H_5)]^-$ and where little if any ion pairing occurs. Under these conditions the $Mo(CO)_3$ fragment has approximate C_{3v} symmetry and two $\nu(CO)$ absorptions are observed. For thf we argued that the spectrum observed [shown in Fig. 7(*a*)] was consistent with a partial dissociation in accordance with equation (1). We

$$[In\{Mo(CO)_3(\eta\text{-}C_5H_5)\}_3] \xrightarrow{\text{thf}} [In(thf)_x\{Mo(CO)_3(\eta\text{-}C_5H_5)\}_2]^+ + [Mo(CO)_3(\eta\text{-}C_5H_5)]^- \quad (1)$$

have now examined this matter in more detail and have discovered that the situation is a little more complicated, although for reasons that were rather unexpected.

We will start by returning to the spectrum obtained for complex **1** in thf [Fig. 7(*a*), Table 6] (spectra for **1** in CH_2Cl_2, toluene and MeCN are given in ref. 1). The two absorptions at low frequency (1789 and 1749 cm^{-1}) are due to the presence of $[Mo(CO)_3(\eta\text{-}C_5H_5)]^-$ but they do not resemble the spectrum of this anion as seen, for example, for **1** in MeCN[1] or for $[N(PPh_3)_2][Mo(CO)_3(\eta\text{-}C_5H_5)]$ in thf (see above) [Fig. 7(*b*)]. Rather, they resemble the lower-frequency absorptions in the spectrum of $K[Mo(CO)_3(\eta\text{-}C_5H_5)]$ [Fig. 7(*c*)] (1899s, 1791s and 1751s cm^{-1}) or $Na[Mo(CO)_3(\eta\text{-}C_5H_5)]$ [Fig. 7(*d*)] (1901s, 1796s and 1748s cm^{-1}). The reason for the difference in the spectra of $[N(PPh_3)_2][Mo(CO)_3(\eta\text{-}C_5H_5)]$ *vs.* $Na/K[Mo(CO)_3(\eta\text{-}C_5H_5)]$ in thf is that in the latter species significant ion pairing occurs between the Na^+ or K^+ cations and the carbonyl oxygens of the $[Mo(CO)_3(\eta\text{-}C_5H_5)]^-$ anion.[28] This effectively lowers the symmetry of the $Mo(CO)_3$ fragment from C_{3v} to C_s and hence three absorptions are seen instead of two. Our initial thoughts were, therefore, that the situation represented in equation (1) was broadly correct but that complex **1**, in thf, might exist in a form in which a carbonyl oxygen of the $[Mo(CO)_3(\eta\text{-}C_5H_5)]^-$ anion was co-ordinated to the indium centre as shown in diagram **G**. As mentioned in the introduction, there was certainly precedent for this type of interaction involving a Group 13 element and a carbonyl oxygen.[8]

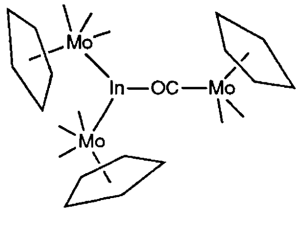

G

Moreover, the remainder of the spectrum of **1** in thf, *i.e.* the absorptions at 1989, 1967 and 1898 cm^{-1}, was similar to spectra observed for other complexes which contain the $InMo_2$ fragment (see refs. 1 and 2 and the following paper).

At this stage we were reasonably confident that we understood the solution-state properties of complex **1** in a variety of solvents. Also, our results were similar to those of others on the solution-state properties of related $[In(ML_n)_3]$ compounds. Thus Hsieh and Mays[29] had observed that $[In\{Mn(CO)_5\}_3]$ was undissociated in CH_2Cl_2 and $CHCl_3$, partially dissociated into $[In(MeCN)_x\{Mn(CO)_5\}_2][Mn(CO)_5]$ in MeCN and fully dissociated into $[In(dmf)_x]^{3+}$ and $3[Mn(CO)_5]^-$ in dimethylformamide (dmf). The cobalt complex $[In\{Co(CO)_4\}_3]$ also dissociates fully in dimethyl sulphoxide (dmso)[30] and our own studies on $[In\{Co(CO)_3(PPh_3)\}_3]$ revealed that, while partial dissociation occurs in MeCN, the fully associated form is present in toluene, CH_2Cl_2 and thf.[4] For $[In\{Fe(CO)_2(\eta\text{-}C_5H_5)\}_3]$, however, we found no evidence for any dissociation in toluene, CH_2Cl_2, thf or MeCN.[3] This tendency of $[In(ML_n)_3]$ species towards ionic behaviour in Lewis-base solvents is not unexpected (see discussion in previous section) and much of indium(III) halide chemistry in solution is ionic. However, the extent of dissociation observed is clearly dependent on the nature of the solvent, and, for a given solvent, on the nature of the metal fragment. It is clear that the more basic solvents promote greater dissociation and it is likely that more detailed studies for a range of compounds in many different solvents would establish a correlation between the extent of dissociation and the basicity or the nucleophilicity of the $[ML_n]^-$ anion. Further comments on this matter are not warranted at this time but we will return to this topic in much more detail in a forthcoming review.[31]

We were forced to think again about the nature of complex **1** in solution when we started to observe some spectra which we had not seen before. A spectrum in acetone is shown in Fig. 7(*e*) which is similar to the spectrum in thf [Fig. 7(*a*)] except that only a single low-frequency absorption is seen, at 1781 cm^{-1}. This is consistent with an ion-separated form $[In(Me_2CO)_x\{Mo(CO)_3(\eta\text{-}C_5H_5)\}_2]^+[Mo(CO)_3(\eta\text{-}C_5H_5)]^-$ since, and with reference to our previous discussion, the single low-frequency absorption is akin to that of $[N(PPh_3)_2][Mo(CO)_3(\eta\text{-}C_5H_5)]$ [Fig. 7(*b*)] but not that of $Na/K[Mo(CO)_3(\eta\text{-}C_5H_5)]$ [Fig. 7(*c*) and (*d*)]. We also observed, however, a spectrum recorded in MeCN that looked almost exactly like the acetone spectrum, *i.e.* Fig. 7(*e*) (data in Table 6) and a spectrum in thf shown in Fig. 7(*f*), which resembles the spectra seen for **1** in CH_2Cl_2 and toluene.[1] At first we thought we had produced a new compound but this notion was quickly dispelled. Samples of complex **1** which gave the thf spectrum shown in Fig. 7(*a*) and samples which gave the spectrum in Fig. 7(*f*) both gave *identical* spectra in CH_2Cl_2 and *identical* spectra in toluene. Moreover, these spectra were exactly the same as those originally reported[1] for **1** in these solvents. We were also able to rule out any concentration effect since both types of spectrum were obtained for a range of concentrations.

The explanation turned out to be simple although unexpected. The observation of either the Fig. 7(*a*) or (*f*) spectrum in thf was found to be dependent on the type of solution infrared cell used, KBr giving the former whilst CaF_2 gave the latter. A single experiment where a solution of complex **1** was divided and one half run in KBr and the other in CaF_2 was enough to confirm this. Moreover, when powdered KBr was added to a thf solution of **1** the resulting spectrum in CaF_2 cells was identical to that shown in Fig. 7(*a*). We suggest, therefore, that in the presence of KBr, **1** reacts in thf to give $[InBr\{Mo(CO)_3(\eta\text{-}C_5H_5)\}_2]$ and $K[Mo(CO)_3(\eta\text{-}C_5H_5)]$, the spectrum in Fig. 7(*a*) being a superposition of the spectra of these two compounds. We have already commented on the similarity between the low-frequency peaks in Fig. 7(*a*) and the spectrum of $K[Mo(CO)_3(\eta\text{-}C_5H_5)]$; the similarity between the remainder of the spectrum and complexes containing the $In\{Mo(CO)_3(\eta\text{-}C_5H_5)\}_2$ fragment has also been mentioned. In CaF_2, **1**, in thf, remains fully associated and the spectrum [Fig. 7(*f*)] resembles those seen in CH_2Cl_2 and toluene.[1] Compound **1** in these latter two solvents gives the same spectrum in both KBr and CaF_2 cells. Hsieh and Mays[10] have reported the infrared spectrum of **1** in $CHCl_3$ which shows strong absorptions at 1976 and 1890 cm^{-1} with weaker signals at 1998, 1911 and 1867 cm^{-1}. These data indicate that **1** is undissociated in this solvent. Published data for the tritungsten–gallium complex **4** are 2020s and 1940s cm^{-1} (C_6H_6)[11] and for the molybdenum analogue, **3**, are 1964s, 1905s and 1889w cm^{-1} (toluene).[12] These data also indicate undissociated forms in these solvents. Our initial thinking about the low-frequency absorption of complex **1** in thf being due to a type **G** structure was unlikely to be correct for another reason. For the complex $[GaPh_3\{W(CO)_3(\eta\text{-}C_5H_5)\}]$[8] the absorption due to the Ga-bonded CO is at much lower frequency, 1642 cm^{-1} (CH_2Cl_2).

The same explanation holds for complex **1** in MeCN. The spectrum given in ref. 1 was obtained in a KBr cell whilst the spectrum which resembles Fig. 7(*e*) was obtained in CaF_2, as was the spectrum of **1** in acetone [Fig. 7(*e*)]. We suggest therefore that **1** exists in MeCN in a similar form to that which we have described for acetone, *i.e.* $[In(MeCN)_x\{Mo(CO)_3(\eta\text{-}C_5H_5)\}_2]^+[Mo(CO)_3(\eta\text{-}C_5H_5)]^-$ (*cf.* $[In\{Mn(CO)_5\}_3]$ in MeCN[29]) and that this is what we observe in CaF_2 cells. However, in KBr a reaction occurs which leads to complete dissociation resulting in solvated indium tribromide and $3K[Mo(CO)_3(\eta\text{-}C_5H_5)]$. The reason why the latter species does not afford a spectrum akin to Fig. 7(*c*) is that in MeCN the K^+ ion is effectively solvated and does not therefore form a close ion pair with the $[Mo(CO)_3(\eta\text{-}C_5H_5)]^-$ anion.[28] Thus a spectrum similar to that of the $N(PPh_3)_2{}^+$ salt in thf [Fig. 7(*b*)] is observed.

Subsequent to our 'discovery' we found a report by Burlitch[32] which described very similar results for a range of mercury complexes, $[Hg(ML_n)_2]$. Specifically, $[Hg\{Co(CO)_4\}_2]$ in dmf showed extensive dissociation in NaCl cells but little if any in CaF_2. In summary, therefore, the choice of infrared solution cell is very important for the types of complexes described herein. All of the spectra reported in ref. 1 were obtained in KBr cells and yet when we started to use CaF_2 cells markedly different spectra were observed, particularly in thf and MeCN. (As we have already mentioned, for CH_2Cl_2 and toluene the choice of cell has little effect.)

We have done little further work on the tritungsten–indium complex **2**. We have observed, however, that samples of **2** gave a spectrum in thf similar to that seen for **1** in Fig. 7(*f*) [ν(CO) 2019w, 1961s, 1922w and 1886s cm^{-1}] in CaF_2; the spectrum reported in ref. 1 was obtained in KBr cells.

For the trichromium–indium complex **8** infrared spectra obtained on solutions derived from crystals of **8** in CaF_2 cells are shown in Fig. 8 (data in Table 6). The important aspect of all these spectra is the presence of two strong, sharp absorptions at around 1955 and 1888 $\pm$ 2 cm^{-1} which, on the basis of our previous discussion for **1**, is consistent with a fully associated structure in solution and with the solid-state structure. The weaker absorptions near 2010 and 1980 $\pm$ 5 cm^{-1} are more prominent than the analogous features seen in the spectra of **1** and **2**[1] but most noteworthy are the absorptions seen at 1774 and 1778 cm^{-1} in the spectra obtained in MeCN and acetone respectively. The signals are due to the presence of $[Cr(CO)_3(\eta\text{-}C_5H_5)]^-$ and therefore indicate that in these solvents **8** is partly dissociated.* Comparisons of the spectra for **8** and **1** in MeCN and acetone, however [Fig. 8(*d*) and (*e*) for **8** and Fig. 7(*e*) for **1**] reveal that **8** dissociates to a slightly lesser extent than **1** in these solvents.

---

* We must be careful how we define 'partly' and 'partially'. In normal English these words are synonymous but in the Chemist's English they are not. For a complete discussion and a nice example see ref. 33. In the present context we define partially dissociated as the situation wherein a complex $[In(ML_n)_3]$ is present as $[In(ML_n)_2]^+[ML_n]^-$ whereas by partly dissociated we imply that some, but not all, of the $[In(ML_n)_3]$ form is dissociated. On the basis of the intensities of the low-frequency signals in the spectra of complex **8** in MeCN and acetone we suggest that the latter description is appropriate in this case.

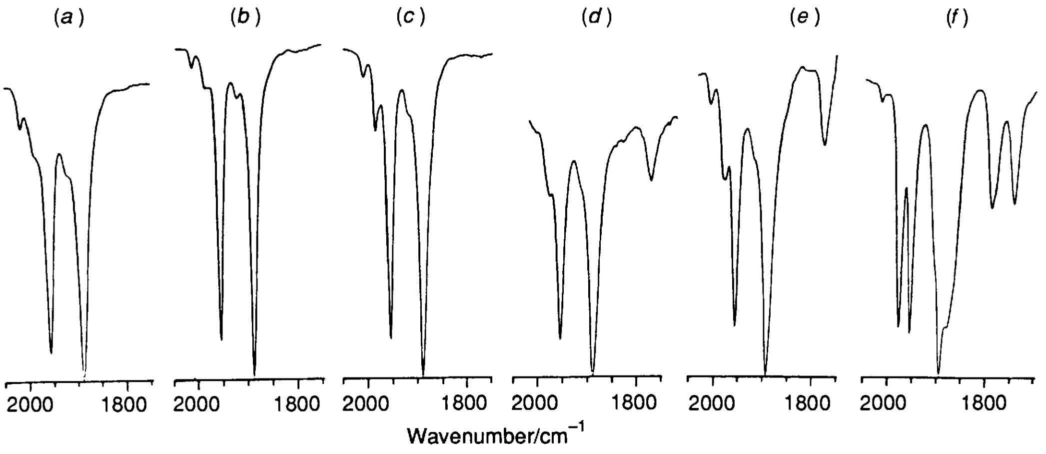

Fig. 8 Infrared spectra in the carbonyl stretching region for complex **8** in CaF_2 cells unless otherwise stated in (*a*) CH_2Cl_2, (*b*) toluene, (*c*) thf, (*d*) MeCN, (*e*) acetone and (*f*) thf, KBr cells

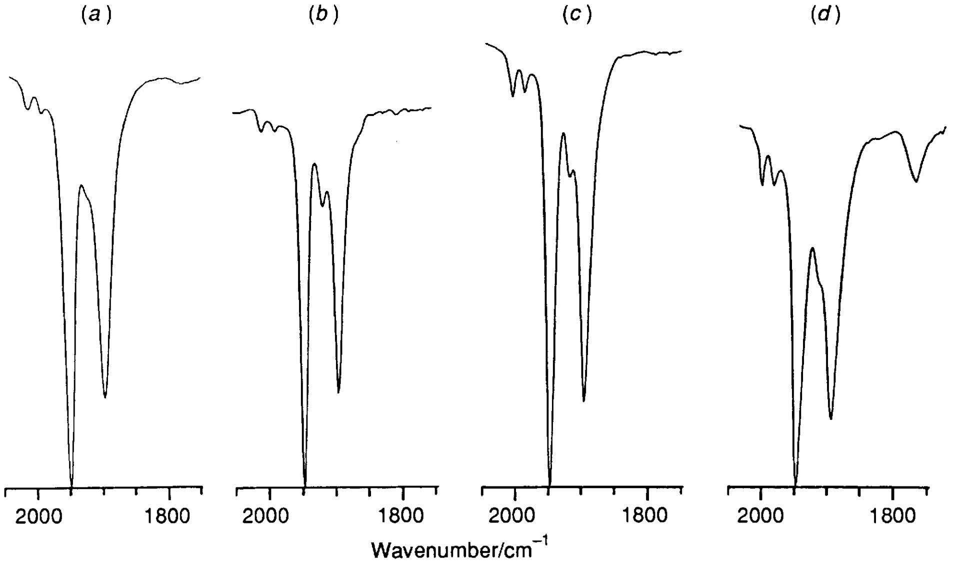

Fig. 9 Infrared spectra in the carbonyl stretching region for complex **5** in CaF_2 cells in (*a*) CH_2Cl_2, (*b*) toluene, (*c*) thf and (*d*) MeCN

The spectrum shown in Fig. 8(*f*) was obtained for complex **8** in thf in KBr cells; clearly the effect we have seen for **1** in thf in CaF_2 cells *vs.* KBr cells is also present for **8**.

The thallium complexes **5** and **6** have previously been reported. Infrared spectra for **5** recorded in CaF_2 cells are shown in Fig. 9 with numerical data in Table 6. All spectra are consistent with an associated structure in solution although a small degree of dissociation is evident in MeCN as judged from the presence of the absorption at 1774 cm^{-1}. Values for **5** in thf are also given in ref. 16 (2006w, 1988w, 1947vs, 1917w and 1895vs cm^{-1}), which are in excellent agreement with our own, in CH_2Cl_2 in ref. 17*a* (1990w, 1952s and 1901s cm^{-1}) and in CS_2 in ref. 17*b* (1973w, 1948s and 1899s cm^{-1}). Infrared data for **6** are available in CH_2Cl_2, toluene and thf[16] and as a KBr disc[14] and for **7** in thf[16] all of which are consistent with an associated structure. A spectrum of **5** in thf obtained in a KBr cell was very similar in appearance to the analogous spectrum of **8** which is shown in Fig. 8(*f*). Clearly complexes **1**, **2**, **5** and **8** react with KBr in thf in the same manner.

Conclusion

We have synthesised and structurally characterised a range of complexes of general formula $[E\{M(CO)_3(\eta\text{-}C_5H_5)\}_3]$ (E = In or Tl, M = Cr or Mo).* For the indium-molybdenum complex we have examined the bonding by EHMO methods and found in particular that In–Mo π bonding is weak. The solution-state properties of these complexes clearly indicate a substantial degree of ionic character reflecting polar In–M bonds, although the precise behaviour is very dependent on the solvent. Further related work is described in the following paper.

Experimental

General Considerations.—All reactions were performed using standard Schlenk techniques under an atmosphere of dry, oxygen-free dinitrogen. All solvents were distilled from appropriate drying agents (sodium–benzophenone for thf, Et_2O, hexane and toluene; CaH_2 for CH_2Cl_2 and MeCN) immediately prior to use. Infrared spectra were recorded on a Nicolet 20 SXB FTIR spectrometer, ^1H and ^{13}C NMR spectra on a Bruker WP 200 spectrometer operating at 200.13 and 50.324 MHz respectively. Microanalytical data were obtained at the University of Newcastle.

All indium and thallium salts were procured commercially and used without further purification. The complexes $[M_2(CO)_6(\eta\text{-}C_5H_5)_2]$ were prepared by the method of Manning and co-workers.[35]

---

* While this work was in progress a report appeared[34a] which described an additional synthetic route to complex **1**: photolysis of $[Mo_2(CO)_6(\eta\text{-}C_5H_5)_2]$ in thf in the presence of indium metal.

Note added at proof: With reference to our discussion of $[E(ML_n)_3]$ complexes we note the recent report of the structure of $[In\{Fe(CO)_4\}_3]^{3-}$.[34b]

Preparations.—[In{Mo(CO)$_3$(η-C$_5$H$_5$)}$_3$] **1**. This was prepared as described in ref. 1.

[In{Cr(CO)$_3$(η-C$_5$H$_5$)}$_3$] **8**. A stirred solution of K[Cr(CO)$_3$(η-C$_5$H$_5$)], derived from sodium–potassium alloy (1:1) (0.3 cm^3) reduction of [Cr$_2$(CO)$_6$(η-C$_5$H$_5$)$_2$] (0.240 g, 0.596 mmol), in thf (20 cm^3) was cooled to 0 °C (ice-bath) and maintained at this temperature. To this was added a solution of InCl$_3$ (0.088 g, 0.397 mmol) in thf (10 cm^3) over a period of a few minutes with continuous stirring. After complete addition, the turbid yellow reaction mixture was allowed to warm to room temperature and was stirred for another 3.5 h. Removal of the solvent by vacuum afforded a dark yellow oily residue which was extracted in CH$_2$Cl$_2$ (30 cm^3) and filtered through Celite. After reduction of the solvent volume to ≈8 cm^3, crystallisation was effected by solvent diffusion with hexane (50 cm^3) at −30 °C over a period of days. This afforded complex **8** as dark orange block-like crystals with typical yields of 40%. These crystals were suitable for X-ray diffraction. NMR [(CD$_3$)$_2$CO]: ^{1}H, δ 5.13 (s, 5 H, C$_5$H$_5$); ^{13}C-{^{1}H}, δ 89.3 (s, C$_5$H$_5$) (Found: C, 39.85; H, 1.90. C$_{24}$H$_{15}$Cr$_3$InO$_9$ requires C, 40.15; H, 2.10%).

[Tl{Cr(CO)$_3$(η-C$_5$H$_5$)}$_3$] **5**. A piece of thallium metal (3 g) was stirred with [Cr$_2$(CO)$_6$(η-C$_5$H$_5$)$_2$] (0.153 g, 0.381 mmol) in toluene (10 cm^3) at room temperature. After 1 h the green solution had turned dark red. Stirring was continued for 5 h. Filtration through Celite followed by removal of the toluene by vacuum afforded a dark red solid. Crystallisation by solvent diffusion from CH$_2$Cl$_2$–hexane mixtures at −30 °C afforded, after 5 d, very dark red crystals in high yield which were suitable for X-ray diffraction. A further batch of crystals was obtained by removal of the solvents from the mother-liquor and recrystallisation from CH$_2$Cl$_2$–hexane mixtures at −30 °C. This synthetic method is essentially the same as one of the methods given in ref. 17.

[Tl{Mo(CO)$_3$(η-C$_5$H$_5$)}$_3$] **6**. A sample of the yellow thallium(I) complex [Tl{Mo(CO)$_3$(η-C$_5$H$_5$)}], prepared by the method of Burlitch and Theyson[16] was dissolved in thf (5 cm^3). A dark red solution formed immediately with concomitant formation of a grey precipitate. After 15 min the thf was removed by vacuum and the dark red residue extracted with CH$_2$Cl$_2$ (10 cm^3) and filtered through Celite. After reduction of the solvent volume of the filtrate to ≈5 cm^3, crystallisation was effected by solvent diffusion using hexane (20 cm^3) at −30 °C over a period of days. This afforded very dark red crystals of complex **6** suitable for X-ray diffraction.

X-Ray Crystallographic Studies.—*Crystal data for compound* **8**. C$_{24}$H$_{15}$Cr$_3$InO$_9$, M_r = 718.18, monoclinic, space group $P2_1/n$, a = 11.088(2), b = 17.282(3), c = 13.787(3) Å, β = 102.94(2)°, U = 2574.8 Å^3 (from 2θ values of 32 reflections in the range 20–25°), Z = 4, D_c = 1.852 g cm^{-3}, $F(000)$ = 1408, μ(Mo-Kα) = 2.124 mm^{-1}, λ = 0.710 73 Å.

Data collection and reduction. Stoe-Siemens diffractometer with graphite monochromator, crystal size 0.38 × 0.46 × 0.35 mm, T = 295 K, $2\theta_{max}$ = 50°. Index ranges: h −13 to 13, k 0–20, l 0–16, with equivalent reflections (k, l < 0), ω–θ scan mode, on-line profile fitting.[36] Of 4759 reflections measured, 4545 were unique and 3643 with $F > 4\sigma_c(F)$ were used for structure determination (R_{int} = 0.032, σ_c from counting statistics only). Data were corrected for Lorentz and polarisation effects, and semiempirical absorption corrections were applied (transmission factors 0.33–0.39). Intensity decay and extinction effects were negligible.

Structure solution and refinement.[37] Isostructural with complex **1** previously reported.[1] Refined with anisotropic thermal motion parameters to minimise $\Sigma w\Delta^2$, $\Delta = |F_o| - |F_c|$, $w^{-1} = \sigma^2(F) = \sigma_c^2(F) + 8 - 26G + 32G^2 - 24S + 18S^2 + 38GS$ ($G = F_o/F_{max}$, $S = \sin\theta/\sin\theta_{max}$).[38] Hydrogen atoms constrained on ring-angle external bisectors with C–H 0.96 Å, U(H) = 1.2U_{eq}(C); for 335 refined parameters, R = 0.030, R' = 0.031, goodness of fit = 1.06. The largest features in the final difference synthesis were close to the heavy atoms. Scattering factors were taken from ref. 39.

Crystal data for complex **1**·thf. C$_{28}$H$_{23}$InMo$_3$O$_{10}$, M_r = 922.12, hexagonal, space group $P\bar{6}2c$, $a = b$ = 12.0511(9), c = 12.2889(9) Å, U = 1545.6 Å^3 (from 2θ values of 36 reflections in the range 20–25°), Z = 2, D_c = 1.981 g cm^{-3}, $F(000)$ = 892, μ(Mo-Kα) = 1.939 mm^{-1}, λ = 0.710 73 Å.

Data collection and reduction. As for complex **8** except crystal size 0.19 × 0.15 × 0.35 mm, T = 240 K, transmission 0.70–0.83, no significant decay. Index ranges: h 0–14, k 0–14, l 0–14, with equivalent reflections (h, k, l < 0). Of 3118 data, 971 were unique and 914 had $F > 4\sigma_c(F)$, R_{int} = 0.019.

Structure solution and refinement. As for complex **8** except atom positions determined by direct methods and difference synthesis $w^{-1} = \sigma_c^2(F) + 1 - 215G + 284G^2 + 24S + 26S^2 + 116GS$. The thf is disordered, one atom located only, all other non-H atoms refined with anisotropic thermal motion parameters; C$_5$H$_5$ ring constrained to give idealised geometry. For 67 refined parameters, R = 0.034, R' 0.026, goodness of fit = 1.19. An isotropic secondary extinction coefficient x refined to 5.4(18) × 10^{-7}, whereby $F'_c = F_c/(1 + xF_c^2/\sin 2\theta)^{\frac{1}{4}}$.

Crystal data for complex **5**. C$_{24}$H$_{15}$O$_9$Cr$_3$Tl, M_r = 807.73, monoclinic, space group $P2_1/n$, a = 11.204(2), b = 17.344(3), c = 13.755(2) Å, β = 103.11(2)°, U = 2603.2 Å^3, Z = 4, D_c = 2.061 g cm^{-3}, $F(000)$ = 1536, μ(Mo-Kα) = 7.475 mm^{-1}.

Data collection and reduction. As for complex **8** except crystal size 0.31 × 0.27 × 0.08 mm, transmission 0.09–0.24, *ca.* 2.6% intensity decay. Of 6183 data, 4598 were unique and 3282 had $F > 4\sigma_c(F)$, R_{int} = 0.0284.

Structure solution and refinement. As for complex **8** except $w^{-1} = \sigma_c^2(F) - 13 + 591G + 1290G^2 - 61S + 150S^2 - 1342GS$. For 334 refined parameters, R = 0.055, R' 0.050, goodness of fit = 1.33.

Crystal data for complex **6a**. C$_{24}$H$_{15}$Mo$_3$O$_9$Tl, M_r = 939.57, monoclinic, space group $P2_1/n$, a = 11.502(5), b = 17.784(7), c = 13.545(6) Å, β = 102.14(4)°, U = 2708.8 Å^3, Z = 4, D_c = 2.304 g cm^{-3}, $F(000)$ = 1752, μ(Mo-Kα) = 7.366 mm^{-1}.

Data collection and reduction. As for complex **8** except crystal size 0.15 × 0.23 × 0.35 mm, T = 240 K, transmission 0.09–0.16. Index ranges h −13 to 13, k 0–21, l 0–16 with equivalent reflections. Of 5966 data, 4793 were unique and 3694 had $F > 4\sigma_c(F)$, R_{int} = 0.0170.

Structure solution and refinement. As for complex **8** except $w^{-1} = \sigma_c^2(F) + 4 + 984G + 36G^2 - 174S + 207S^2 - 1173GS$. For 334 refined parameters, R = 0.0477, R' 0.054, goodness of fit = 1.138.

Additional material available from the Cambridge Crystallographic Data Centre comprises H-atom coordinates, thermal parameters and remaining bond lengths and angles.

Extended-Hückel Molecular Orbital Calculations.—Molecular orbital calculations were of the extended-Hückel type[40] using the program ICON8 with fragment MO analysis.[41] The Hückel constant was set to 1.75 and weighted H_{ij} (modified Helmholz–Wolfsberg formula)[42] were used throughout. Parameters for the calculations were taken from ref. 43 except for those for indium which were taken from ref. 44.

As mentioned in the Results and Discussion, the structure of complex **1** on which the calculations were carried out was derived from the coordinates for **1** given in ref. 1 but averaged to give molecular C_{3h} symmetry. Some time after the calculations were done the structure of **1**·thf was solved in which the molecule of **1** has precise crystallographic C_{3h} symmetry. The only important difference between this later structure and the averaged structure used in the calculation is the In–Mo bond length, 2.878 for **1** *vs.* 2.855 Å for **1**·thf. When the calculations were repeated with the shorter bond length the effect on the orbital energies was negligible.

Acknowledgements

We thank the SERC for a studentship (to L. M. C.) and financial support for the X-ray facilities. N. C. N. and T. B. M. also thank the Royal Society and Natural Sciences and Engineering Research Council (Canada) for funds which have supported our collaboration on the EHMO calculational work. N. C. N. also thanks the Royal Society for additional supporting funds.

References

1 L. M. Clarkson, W. Clegg, N. C. Norman, A. J. Tucker and P. M. Webster, *Inorg. Chem.*, 1988, **27**, 2653.
2 L. M. Clarkson, N. C. Norman and L. J. Farrugia, *J. Organomet. Chem.*, 1990, **390**, C10.
3 N. C. Norman and P. M. Webster, *Z. Naturforsch., Teil B*, 1989, **44**, 91.
4 L. M. Clarkson, K. McCrudden, N. C. Norman and L. J. Farrugia, *Polyhedron*, 1990, **9**, 2533.
5 L. M. Clarkson, N. C. Norman and L. J. Farrugia, *Organometallics*, 1991, **10**, 1286.
6 N. A. Compton, R. J. Errington and N. C. Norman, *Adv. Organomet. Chem.*, 1990, **31**, 91.
7 J. M. Burlitch and R. B. Petersen, *J. Organomet. Chem.*, 1970, **24**, C65.
8 J. M. Burlitch, M. E. Leonowicz, R. B. Petersen and R. E. Hughes, *Inorg. Chem.*, 1979, **18**, 1097.
9 A. T. T. Hsieh and M. J. Mays, *Inorg. Nucl. Chem. Lett.*, 1971, **7**, 223.
10 A. T. T. Hsieh and M. J. Mays, *J. Organomet. Chem.*, 1972, **37**, 9.
11 A. J. Conway, P. B. Hitchcock and J. D. Smith, *J. Chem. Soc., Dalton Trans.*, 1975, 1945.
12 J. N. St. Denis, W. Butler, M. D. Glick and J. P. Oliver, *J. Organomet. Chem.*, 1977, **129**, 1.
13 B. Walther and C. Rockstroh, *J. Organomet. Chem.*, 1972, **44**, C4; B. Walther, H. Albert and A. Kolbe, *J. Organomet. Chem.*, 1978, **145**, 285.
14 R. B. King, *Inorg. Chem.*, 1970, **9**, 1936.
15 J. Rajaram and J. A. Ibers, *Inorg. Chem.*, 1973, **12**, 1313.
16 J. M. Burlitch and T. W. Theyson, *J. Chem. Soc., Dalton Trans.*, 1974, 828.
17 (*a*) S. E. Pedersen and W. R. Robinson, *Inorg. Chem.*, 1975, **14**, 2365; (*b*) see also, P. Hackett, P. S. O'Neill and A. R. Manning, *J. Chem. Soc., Dalton Trans.*, 1974, 1625.
18 B. Nuber, W. Schatz and M. L. Ziegler, *Z. Naturforsch., Teil B*, 1990, **45**, 508.
19 (*a*) R. Guilard, A. Tabard, A. Zrineh and M. Ferhat, *J. Organomet. Chem.*, 1990, **389**, 315; (*b*) P. Richard, A. Zrineh, R. Guilard, A. Habbou and C. Lecomte, *Acta Crystallogr., Sect. C*, 1989, **45**, 1224; (*c*) C. Lecomte, A. Habbou, P. Mitaine, P. Richard and R. Guilard, *Acta Crystallogr., Sect. C*, 1989, **45**, 1226; (*d*) R. Guilard, A. Zrineh, M. Ferhat, A. Tabard, P. Mitaine, C. Swistak, P. Richard, C. Lecomte and K. M. Kadish, *Inorg. Chem.*, 1988, **27**, 697; (*e*) R. Guilard, P. Mitaine, C. Moise, C. Lecomte, A. Boukhris, C. Swistak, A. Tabard, D. Lacombe, J.-L. Cornillon and K. M. Kadish, *Inorg. Chem.*, 1987, **26**, 2467; see also R. Guilard and K. M. Kadish, *Comments Inorg. Chem.*, 1988, **7**, 287.
20 M. L. H. Green, P. Mountford, G. J. Smout and S. R. Speel, *Polyhedron*, 1990, **9**, 2763.
21 H. Behrens, M. Moll, E. Sixtus and G. Thiele, *Z. Naturforsch., Teil B*, 1977, **32**, 1109.
22 W. R. Robinson and D. P. Schussler, *Inorg. Chem.*, 1973, **12**, 848.
23 J. M. Cassidy and K. H. Whitmire, *Inorg. Chem.*, 1989, **28**, 2494.
24 G. Huttner, U. Weber, B. Sigwarth, O. Sheidsteger, H. Lang and L. Zsolnai, *J. Organomet. Chem.*, 1985, **282**, 331.
25 M. Herberhold, D. Reiner and D. Neugelbauer, *Angew. Chem., Int. Ed. Engl.*, 1983, **22**, 59.
26 See also, P. Kubacek, R. Hoffmann and Z. Havlas, *Organometallics*, 1982, **1**, 180.
27 M. Veith and K. Kunze, *Angew. Chem., Int. Ed. Engl.*, 1991, **30**, 95.
28 M. Y. Darensbourg, *Prog. Inorg. Chem.*, 1985, **33**, 221.
29 A. T. T. Hsieh and M. J. Mays, *Chem. Commun.*, 1971, 1234; *J. Chem. Soc., Dalton Trans.*, 1972, 516.
30 W. R. Robinson and D. P. Schussler, *J. Organomet. Chem.*, 1971, **30**, C5.
31 L. M. Clarkson and N. C. Norman, unpublished work.
32 J. M. Burlitch, *J. Am. Chem. Soc.*, 1969, **91**, 4563.
33 R. Schoenfeld, *The Chemist's English*, VCH, Weinheim, 1985.
34 (*a*) D. L. Thorn, *J. Organomet. Chem.*, 1991, **405**, 161; (*b*) V. G. Albano, M. Cané, M. C. Iapalucci, G. Longoni and M. Monari, *J. Organomet. Chem.*, 1991, **407**, C9.
35 R. Birdwhistell, P. Hackett and A. R. Manning, *J. Organomet. Chem.*, 1978, **157**, 239.
36 W. Clegg, *Acta Crystallogr., Sect. A*, 1981, **37**, 22.
37 G. M. Sheldrick, SHELXTL, An integrated system for solving, refining and displaying crystal structures from diffraction data, University of Göttingen, 1985, revision 5.
38 Wang Hong and B. E. Robertson, *Structure and Statistics in Crystallography*, ed. A. J. C. Wilson, Adenine Press, New York, 1985, pp. 125–136.
39 *International Tables for X-Ray Crystallography*, Kynoch Press, Birmingham, 1974, vol. 4, pp. 99, 149.
40 R. Hoffmann, *J. Chem. Phys.*, 1963, **39**, 1397; R. Hoffmann and W. N. Lipscomb, *J. Chem. Phys.*, 1962, **36**, 2179; **37**, 2872.
41 A. Rossi, J. Howell, D. Wallace, K. Haraki and R. Hoffmann, Program ICON 8, Quantum Chemistry Program Exchange no. 517, 1986, vol. 6, p. 100.
42 J. H. Ammeter, H.-B. Burgi, J. C. Thibeault and R. Hoffmann, *J. Am. Chem. Soc.*, 1978, **100**, 3686.
43 R. H. Summerville and R. Hoffmann, *J. Am. Chem. Soc.*, 1976, **98**, 7240.
44 E. Canadell, O. Eisenstein and J. Rubio, *Organometallics*, 1984, **3**, 759.

Received 6th *March* 1991; *Paper* 1/01078F